MATERIALS CHEMISTRY FRONTIERS

RESEARCH ARTICLE

View Article Online
View Journal | View Issue

Cite this: *Mater. Chem. Front.*, 2022, **6**, 1623

Efficient red organic LEDs *via* the combination of an exciplex host and micro-cavity†

Jiao-Yang Li,‡[a] Ya-Kun Wang,‡*[a] Jun-Gui Zhou,[a] Wei He,[a] Xiao-Hao Dong,[a] Chuan Zhang,[b] Xiao-Bo Shi,[b] Liang-Sheng Lia *[abc] and Man-Keung Fung *[abc]

Received 7th March 2022,
Accepted 24th April 2022

DOI: 10.1039/d2qm00203e

rsc.li/frontiers-materials

Exploring exciplexes as the host in organic light-emitting diodes (OLEDs) has attracted extensive attention because of the low driving voltage and high efficiency. However, conventional exciplex-host-based bottom-emission still shows undesirable efficiencies, especially in the red emission channels, due to energy gap law. We here propose exciplex-host-based top-emitting devices to achieve breakthrough efficiency in red light-emitting devices. We optimize the exciplex hosts to maximize energy transfer to the emitting dyes and the cavity length and reflective electrodes to achieve efficient red organic LEDs. We report a current efficiency of 99.7 cd A^{-1} for a red OLED with an electroluminescence (EL) peak at 604 nm (full width at half maximum of 32 nm); these efficiencies are the best in red OLEDs, especially with a narrow EL spectrum. This work offers a new strategy to achieve high efficiency and high color-purity LEDs simultaneously.

Exciton utilization, a key factor in achieving high external quantum efficiency, has been attracting continuous attention in light-emitting materials.[1–5] Nearly 100% exciton utilization and internal quantum efficiency have been achieved by either introducing heavy atoms to form phosphorescent dyes or manipulating the singlet–triplet energy splitting (ΔE_{st}) to achieve thermally activated delayed fluorescence (TADF). For TADF materials, minimizing electron exchange energy is the key parameter that allows efficient repopulation from the emission-forbidden triplet states to the emissive singlet states, which generally needs separation of the highest occupied molecular orbital (HOMO) and lowest unoccupied molecular orbital (LUMO). Benefiting from the sophisticated molecular designs, OLEDs based on intramolecular TADF emitters have been reported.[6–8] However, the challenges for the TADF-based OLED devices have just begun. The sophisticated molecular designs complicate the syntheses, which might hamper advancements in commercialization.

In addition to the intramolecular TADF system, mixing a donor with an acceptor to form an intermolecular charge transfer exciplex also produces the TADF effect.[9–13] There have been concerted studies by optimizing energy-matched hole-dominant and electron-dominant moieties to form exciplex-type hosts for phosphorescent OLEDs.[14] The long-range Förster energy transfer in an exciplex host allows the doped emitter to be at a low concentration, helping the OLEDs to achieve a low driving voltage and reduced efficiency roll-off.[15] For example, Kim *et al.* reported exciplex-host-based phosphorescent OLEDs with a high efficiency.[16] However, the broad EL spectrum with FWHM >70 nm may need further spectral engineering for those applications that require high color purity.

Strategies to narrow the emission and further improve the luminous efficiency have been demonstrated by using multi-resonance (MR) materials; narrowing FWHM below 30 nm and achieving over 30% quantum efficiency were reported in blue OLEDs, but the asymmetric emission and long emission tail provoke other challenges because the FWHM is insufficient to express its color purity.[17,18] There have been a few studies on the light coupling of TADF- or exciplex-based green OLEDs with a narrow EL.[36] It is expected that the optical power dissipation of their green emissions will be different to that of other emitters.[37]

We here propose a strategy by screening an exciplex host and combining it with a top-emitting architecture to push the efficiency of red emission to the limit and narrow the FWHM at the same time; the optimized exciplex host ensures effective

[a] *Institute of Functional Nano & Soft Materials (FUNSOM), Jiangsu Key Laboratory for Carbon-Based Functional Materials & Devices, Soochow University, 199 Ren'ai Road, Suzhou, 215123, Jiangsu, P. R. China. E-mail: wangyakun@suda.edu.cn, lsliao@suda.edu.cn, mkfung@suda.edu.cn; Fax: +86-512-65882846; Tel: +86-512-65880951*

[b] *Institute of Organic Optoelectronics (IOO), Jiangsu Industrial Technology Research Institute (JITRI), 1198 Fenhu Dadao, Wujiang, Suzhou, Jiangsu, P. R. China*

[c] *Macao Institute of Materials Science and Engineering (MIMSE), MUST-SUDA Joint Research Center for Advanced Functional Materials, Zhuhai MUST Science and Technology Research Institute, Macau University of Science and Technology, Taipa 999078, Macau, China*

† Electronic supplementary information (ESI) available. See DOI: https://doi.org/10.1039/d2qm00203e

‡ These authors contributed equally to this work.

energy transfer and low driving voltages; the micro-cavity engineering with top-emitting techniques ensures narrow FWHM and high performance. We achieve an efficient red OLED with a high-current efficiency of 99.7 cd A^{-1}. The efficiency roll-off is also suppressed because of the well-designed exciplex host. The devices, upon optimization of the micro-cavity length, exhibit a much narrower FWHM of 32 nm, which is over 2.5-fold narrower than that of the conventional devices (80 nm). These performances are the most superior among both solution-processed and vacuum-evaporated red OLEDs.

The potential of utilizing exciplexes as the host has been witnessed by delicate materials design *via* tuning the hole/electron transporting ability and regulating the energy level.[19,20] However, these studies were mostly on bottom-emitting devices, which emitted light from the transparent indium tin oxide (ITO). The bottom-emitting devices feature weak micro-cavity effects because of the less reflectivity of the ITO and the weak optical interference coming from the thick Al cathode. The two-beam interferences in the bottom emitting devices (Ref-Be) show a weak micro-cavity effect and large FWHM because of the less ability to couple the light and redistribute the density of optical modes. Replacing the transparent ITO with a highly reflective anode and the thick Al with a semi-transparent cathode could greatly enhance the micro-cavity effect.[21–25] This Fabry–Perot mirror-like top-emitting architecture featuring two reflective electrodes exhibits a strong micro-cavity effect because of the existence of multiple reflections and extra light interferences.[26–29] Furthermore, this multiple optical interference affects the light-emitting pathways and helps increase light out-coupling, thus increasing the efficiency.[30–35]

To use an exciplex host in the top-emitting structures (Ex-Te), delicate design of the exciplex host and the micro-cavity length are keys to simultaneously achieve high device performance and narrow FWHM. We first screen different kinds of exciplex host materials and investigate their energy transfer properties when used as the host for red emitters. We chose exciplex host systems based on 4,6-bis[3,5-(dipyrid-4-yl)phenyl]-2-methylpyrimidine (B4PyMPM) as the electron acceptor moiety because of its deep HOMO and LUMO energy, which are in favor of hole-blocking and are easy to match with the host materials to form an exciplex. For the donor moiety, we used two typical host materials, 1,3-di(9*H*-carbazol-9-yl)benzene (mCP) and 4,4′-bis(*N*-carbazolyl)biphenyl (CBP). We investigated the emission of CBP:B4PyMPM and mCP:B4PyMPM and observed a 20 nm shift in the former exciplex, as shown in the photoluminescence spectra in Fig. 1a. This redshift is important because when we use it as the host in OLEDs, the energy transfer will be more complete with less exciton loss. Furthermore, the triplet energy of the CBP:B4PyMPM exciplex is estimated to be 2.70 eV, which is sufficient to suppress the exciton loss to the adjacent functional materials and confine all the excitons in the emitter.

We first fabricated conventional bottom emitting devices to verify the emission profile of the red phosphorescent OLEDs using the following architecture: ITO/1,4,5,8,9,11-hexaazatriphenylene-hexacarbonitrile (HAT-CN) (10 nm)/1,1-bisy[4-[*N*,*N*-di(*p*-tolyl)amino]phenyl]cyclohexane (TAPC) (40 nm)/tris(4-(9*H*-carbazol-9-yl)phenyl)amine (TCTA) (10 nm)/host (20 nm)/B4PyMPM (50 nm)/Liq (2 nm)/Al. The device structure is shown in Fig. 1b. We chose commercially available bis(2-methyldibenzo-[*f*,*h*]quinoxaline) (acetylacetonate) iridium(III) [Ir(MQD)2(acac)] as the emitter because of its desirable emission wavelength and high photoluminescence quantum yield. As expected, its EL shows a wide FWHM of 80 nm (Fig. 1c), which is consistent with the values in the literature.

In both the bottom and top-emitting devices, the spectral width is affected by the optical interference and micro-cavity effect. We next fabricated top-emitting devices as follows: reflective anodes/HAT-CN (10 nm)/TAPC (220 nm)/TCTA (10 nm)/CBP:B4PyMPM:Ir(MDQ)2acac (20 nm)/B4PyMPM (40 nm)/4,7-diphenyl-1,10-phenanthroline (Bphen):Yb (10 nm)/Yb (2 nm)/Ag (20 nm)/Capping layer (CPL). We basically used the same structure as in the bottom-emitting device except replacing the ITO and Al with two reflective anodes. For the reflective anodes, three kinds of electrodes were utilized, namely, ITO, indium zinc oxide (IZO) and aluminum doped zinc oxide (AZO). We compared the reflectivity, sheet resistance and work function of ITO/Ag/ITO, IZO/Ag/IZO and AZO/Ag/AZO to find out the most

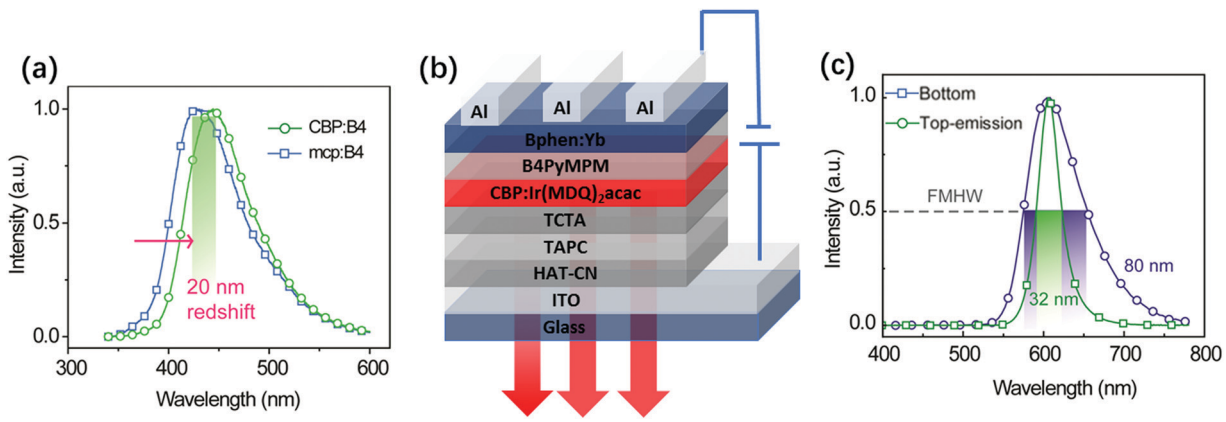

Fig. 1 (a) PL spectra of CBP: B4PyMPM and mCP:B4PyMPM in films at 300 K. (b) Device structure of the bottom-emitting device. (c) Normalized EL spectra of the top-emitting and bottom-emitting devices.

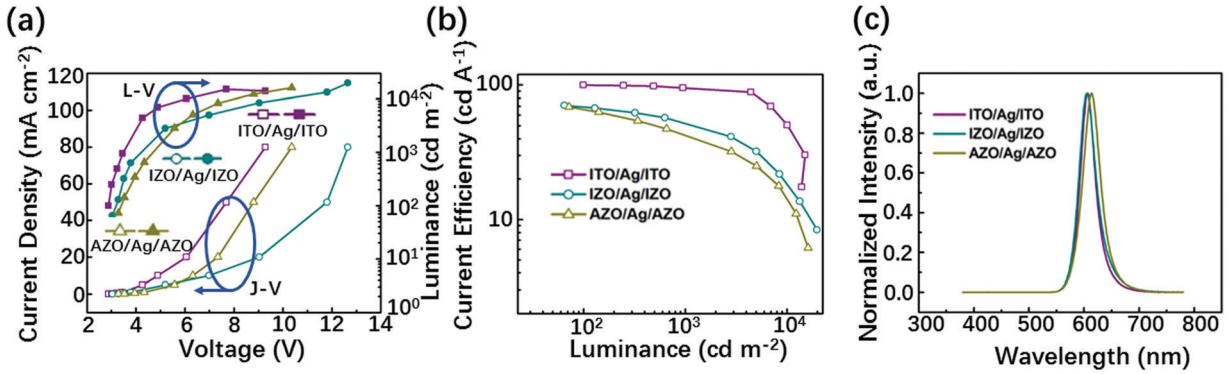

Fig. 2 (a) Current density and luminance *vs.* voltage; (b) current efficiency *vs.* luminance; and (c) normalized EL spectra of Ex-Te devices based on ITO/Ag/ITO, IZO/Ag/IZO, AZO/Ag/AZO anodes.

appropriate anode for the present top-emitting red OLEDs. Among the three anodes, the ITO/Ag/ITO anode provides the highest reflectivity of 98.7% (at 608 nm) and work function of 4.8 eV (Fig. S1 and Table S1, ESI†). To compare the device performance based on different reflective anodes, we fabricated a device in which the TAPC thickness was 220 nm. In Fig. 2, among all the reflective anodes, ITO/Ag/ITO shows the best performance because of its reflectivity of over 98% in the red region and appropriate work function. The semi-transparent Yb/Ag cathode gives ~60% reflectivity to ensure multiple optical interferences and efficient micro-cavity effects and ~40% transmittance to ensure light emitting from the cathode effectively (Fig. S1c, ESI†). In addition to reflectivity, we optimized the composition and thickness of both the anodes and cathodes to minimize the sheet resistance and obtained a low sheet resistance of 0.39 Ω $\square^{-1}$ and 3.0 Ω $\square^{-1}$ for ITO/Ag/ITO and Yb/Ag, respectively (Fig. S1b, ESI†). These low sheet resistances help lower the charge injection barrier and facilitate charge transport. We further deposited a CPL on top of the cathode to enhance the strength of optical interference and the light outcoupling efficiency. With such an enhancement of the micro-cavity effect, we finally observed a much reduced FWHM of 32 nm, which is over 2.5-fold narrower than that of the conventional CPB-based bottom-emitting devices (Fig. 1c). In Fig. S1f (ESI†), ITO/Ag/ITO shows better carrier transport ability in a hole-only device. These results suggest that the micro-cavity was well designed, showing a great potential in achieving high-color-purity OLEDs.

We next performed optical simulation (Lumerical FDTD Solutions) to provide guidance in optimizing the micro-cavity effect and achieving high device performance. To ensure the accuracy of the simulation results, optical parameters for each functional layer were measured using an ellipsometer. For the simulation of the transmittance for the semi-transparent cathode (TC), a plane wave was used as the light source. Since the excitons formed by the combination of holes and electrons in the devices are very close to the dipole model, one dipole

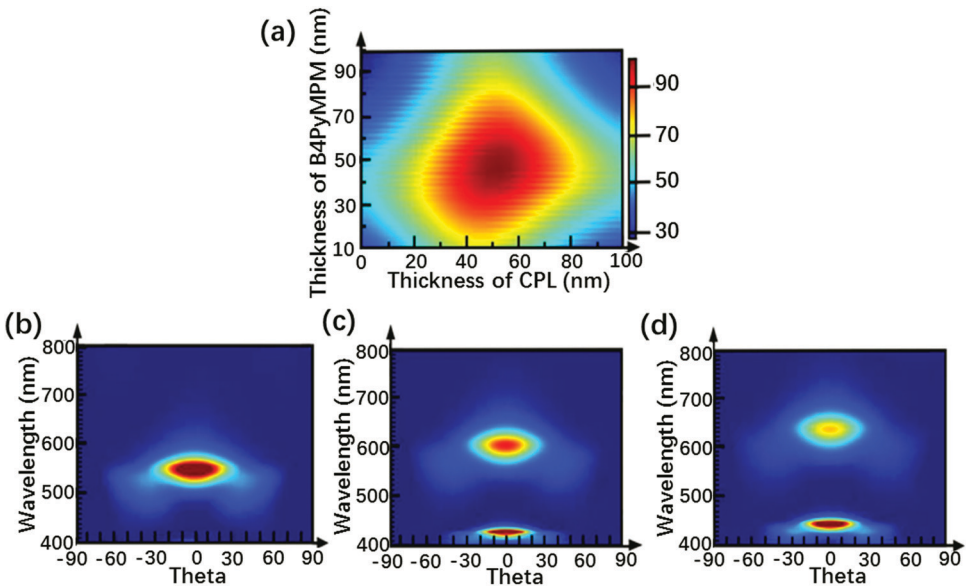

Fig. 3 (a) Simulated optical transmittance intensities as a function of B4PyMPM and CPL thicknesses for light propagation. (b–d) Far-field radiation characteristics of various devices based on different TAPC thicknesses: 180 nm, 220 nm and 240 nm.

with three directions (x, y, z) was selected as the light source for the simulation of far-field E^2 intensity. Thickness dependence of the B4PyMPM and CPL layers as a function of optical transmittance of B4PyMPM/Bphen:Yb/Yb/Ag/CPL was numerically simulated for light propagation at an emission wavelength of 608 nm by the finite difference time domain (FDTD) method. As shown in Fig. 3a, the optimized theoretical thicknesses of CPL and B4PyMPM layers are 40–65 nm and 35–65 nm, respectively. To further analyze how the thickness of TAPC affects the device efficiency and the EL spectra of OLEDs, we used the FDTD method to simulate the far-field radiation characteristics of OLEDs based on various TAPC thicknesses. The far-field radiation characteristics are mainly the relationship between the far-field E^2 intensity, emission wavelength and the observation angle. Fig. 3b is the far-field radiation characteristic image of the device with a 180 nm thick TAPC. In the range of 530–570 nm, the electric-field intensity is the highest. As the thickness of TAPC increases to 240 nm, the range of electric-field intensity is red shifted with a decrease of intensity, while the electric-field intensity for the blue wavelength region is enhanced due to the interference effect (Fig. 3c and d). Accordingly, the result shows that OLEDs with a 220 nm thick TAPC has beneficial effects for red emission.

To consolidate the above simulation result, we investigated the micro-cavity strength by comparing the angular-dependent EL spectra with the Lambertian profile. We found that the EL profiles of bottom-emitting devices suit the Lambertian-like emission pattern, which suggests that there is a weak micro-cavity effect (Fig. 4a). By contrast, the top-emitting LEDs with different thicknesses of TAPC show a narrower emission profile (Fig. 4b) and a larger derivation from the standard Lambertian profile (Fig. 4c). The devices with 180 nm and 240 nm TAPC show similar angular emission profiles and strong micro-cavity effect. These strong micro-cavity effects coincide with the narrow EL spectra; however, their emission wavelengths were deviated from the original wavelength as indicated from the bottom-emitting device. However, the 220 nm thick TAPC device shows moderate microcavity effects and the EL peak perfectly overlaps with that of the bottom-emitting device. Remarkably, it exhibits a narrower EL spectrum with FWHM of only 32 nm, implying that there is an optimal micro-cavity length and device thickness in achieving a narrow and unshifted EL spectrum. Its angular-dependent EL spectra are shown in Fig. S2a (ESI†).

We then fabricated top-emitting red organic LEDs with TAPC thicknesses of 180 nm, 220 nm and 240 nm so as to optimize the micro-cavity length and substantiate the optical simulation results. The device structure and its energy level diagram are shown in Fig. 5a and b, respectively. The device performance based on 180 nm and 240 nm thick TAPC shows maximum current efficiencies of 72.9 cd A^{-1} and 36 cd A^{-1}, respectively. In accordance with the optical simulations, the device with 220 nm thick TAPC exhibits a maximum current efficiency of 99.7 cd A^{-1} (Fig. 5c); these efficiencies represent the highest among all reported red OLEDs without using any external outcoupling techniques, particularly for a device with an emission width as narrow as 32 nm in FWHM (Fig. 1c). For comparison, the exciplex-based and conventional CPB-based bottom-emitting devices only exhibit a maximum current efficiency of 31.8 cd A^{-1} and 28.6 cd A^{-1}, respectively (Fig. 5d). Furthermore, benefiting from the exciplex host and well-designed 'exciplex host' device architecture, the efficiency roll-off was also suppressed in the 220 nm thick TAPC device: the current efficiency maintains 97.8 cd A^{-1} and 89.1 cd A^{-1} at 500 cd m^{-2} and 4000 cd m^{-2}, respectively. We also calculated the EQE based on the angular distribution of the EL intensity as shown in Fig. 4. The EQEs for the 220 nm thick TAPC device and the corresponding bottom-emitting device were 23.3% and 17.7%, respectively.

In summary, we have demonstrated a promising strategy to achieve high-efficiency red OLEDs with a narrow EL profile. We take the advantages of using an exciplex host in reducing the driving voltage, enhancing the luminous efficiency and suppressing the efficiency roll-off and engineering the micro-cavities in narrowing the EL spectrum of top-emitting red OLEDs. Our experimental results agree very well with the optical simulations, in which our red OLED exhibited a very high current efficiency of 99.7 cd A^{-1} with a narrow EL

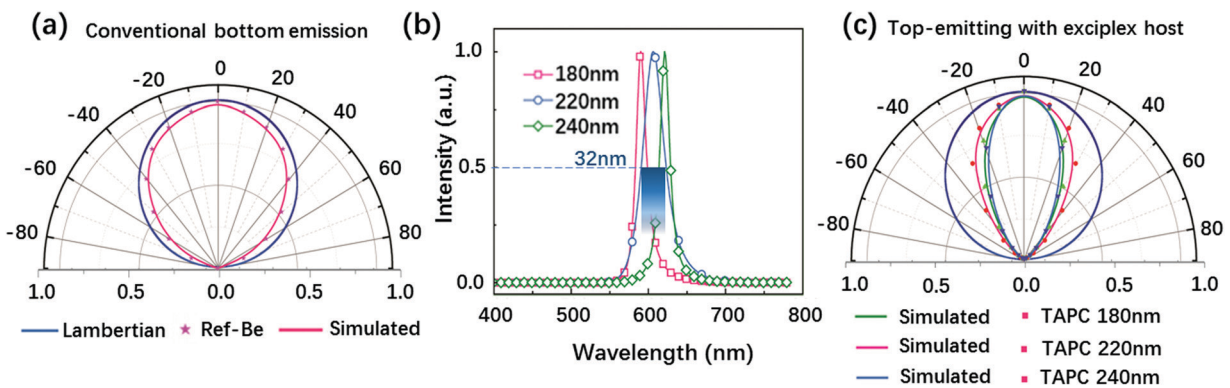

Fig. 4 (a) Experimental (dot) and simulated (line) radiant intensity profiles of conventional Ref-Be with CBP host device. (b) Normalized EL spectra of the Ex-Te with exciplex host device based on different TAPC thicknesses. (c) Experimental (dot) and simulated (line) radiant intensity profiles of Ex-Te with exciplex host devices with 180 nm, 220 nm, and 240 nm TAPC.

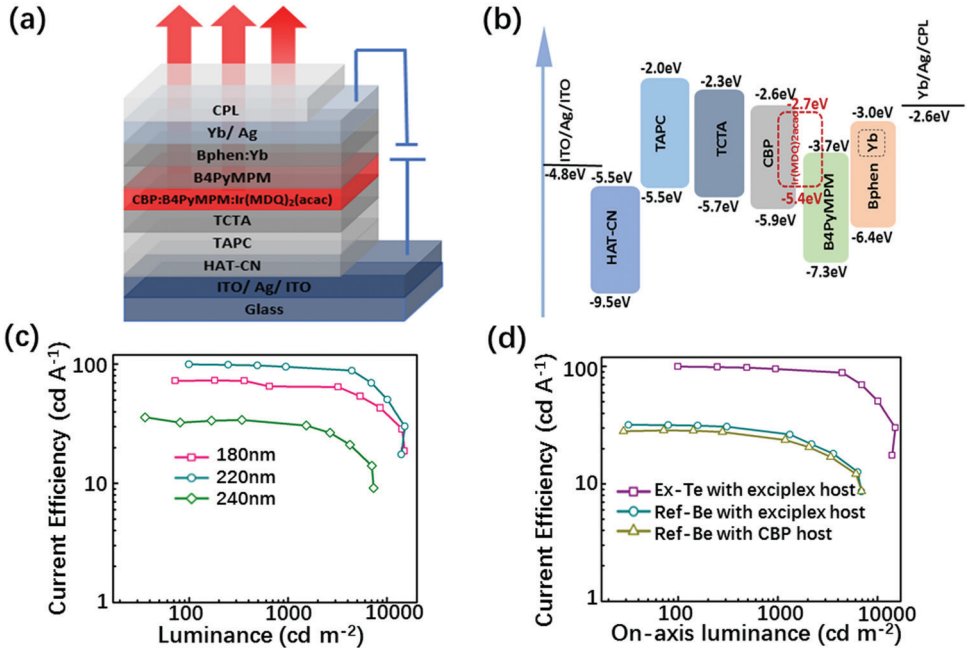

Fig. 5 (a) Device structure of the Ex-Te device. (b) Energy level diagram of the Ex-Te device. (c) Current efficiency *vs.* luminance of the Ex-Te device based on different TAPC thicknesses. (d) Current efficiency *vs.* on-axis luminance of the Ex-Te with exciplex host, Ref-Be with exciplex host and Ref-Be with CBP host devices.

spectrum of only 32 nm in FWHM. This work paves a path for red OLED lighting to be used in automobile taillights and photobiomodulation therapy which require high brightness and excellent color purity.

Conflicts of interest

There are no conflicts to declare.

Acknowledgements

Authors Jiao-Yang Li and Ya-Kun Wang contributed equally to this work. This work is supported by the National Natural Science Foundation of China (61875144), China Postdoctoral Science Foundation (2021M690114 and 2021TQ0230), the Science and Technology Development Fund, Macau SAR (0051/2021/A), the Suzhou Key Laboratory of Functional Nano & Soft Materials, Collaborative Innovation Center of Suzhou Nano Science & Technology, the 111 Project, and Joint International Research Laboratory of Carbon-Based Functional Materials and Devices.

References

1 Z. Wu, N. Sun, L. Zhu, H. Sun, J. Wang, D. Yang, X. Qiao, J. Chen, S. M. Alshehri, T. Ahamad and D. Ma, Achieving Extreme Utilization of Excitons by an Efficient Sandwich-Type Emissive Layer Architecture for Reduced Efficiency Roll-Off and Improved Operational Stability in Organic Light-Emitting Diodes, *ACS Appl. Mater. Interfaces*, 2016, **8**, 3150–3159.

2 J. Chen, W. Liu, C. Zheng, K. Wang, K. Liang, Y. Shi, X. Ou and X. Zhang, Coumarin-based Thermally Activated Delayed Fluorescence Emitters with High External Quantum Efficiency and Low Efficiency Roll-off in the Devices, *ACS Appl. Mater. Interfaces*, 2017, **9**, 8848–8854.

3 B. Liang, J. Wang, Z. Cheng, J. Wei and Y. Wang, Exciplex-Based Electroluminescence: Over 21% External Quantum Efficiency and Approaching 100 lm/W Power Efficiency, *J. Phys. Chem. Lett.*, 2019, **10**, 2811–2816.

4 S. Chen, L. Deng, J. Xie, L. Peng, L. Xie, Q. Fan and W. Huang, Recent Developments in Top-Emitting Organic Light-Emitting Diodes, *Adv. Mater.*, 2010, **22**, 5227–5239.

5 K. T. Ly, R. Chen-Cheng, H. Lin, Y. Shiau, S. Liu, P. Chou, C. Tsao, Y. Huang and Y. Chi, Near-infrared organic light-emitting diodes with very high external quantum efficiency and radiance, *Nat. Photonics*, 2017, **11**, 63–68.

6 C. C. Peng, S. Y. Yang, H. C. Li, G. H. Xie, L. S. Cui, S. N. Zou, C. Poriel, Z. Q. Jiang and L. S. Liao, Highly Efficient Thermally Activated Delayed Fluorescence via an Unconjugated Donor–Acceptor System Realizing EQE of Over 30%, *Adv. Mater.*, 2020, **32**, 2003885.

7 Y. L. Zhang, Q. Ran, Q. Wang, Y. Liu, C. Hänisch, S. Reineke, J. Fan and L. S. Liao, High-Efficiency Red Organic Light-Emitting Diodes with External Quantum Efficiency Close to 30% Based on a Novel Thermally Activated Delayed Fluorescence Emitter, *Adv. Mater.*, 2019, **31**, 1902368.

8 J. X. Chen, K. Wang, Y. F. Xiao, C. Cao, J. H. Tan, H. Wang, X. C. Fan, J. Yu, F. X. Geng, X. H. Zhang and C. S. Lee, Thermally Activated Delayed Fluorescence Warm White

Organic Light Emitting Devices with External Quantum Efficiencies Over 30%, *Adv. Funct. Mater.*, 2021, **31**, 2101647.

9 M. Sarma and K. Wong, Exciplex: An Intermolecular Charge-Transfer Approach for TADF, *ACS Appl. Mater. Interfaces*, 2018, **10**, 19279–19304.

10 W. Liu, J. Chen, C. Zheng, K. Wang, D. Chen, F. Li, Y. Dong, C. Lee, X. Ou and X. Zhang, Novel Strategy to Develop Exciplex Emitters for High Performance OLEDs by Employing Thermally Activated Delayed Fluorescence Materials, *Adv. Funct. Mater.*, 2016, **26**, 2002–2008.

11 L. Chen, J. Lv, S. Wang, S. Shao and L. Wang, Dendritic Interfacial Exciplex Hosts for Solution-Processed TADF-OLEDs with Power Efficiency Approaching 100 lm W^{-1}, *Adv. Opt. Mater.*, 2021, **9**, 20.

12 T. Lin, M. Sarma, Y. Chen, S. Liu, K. Lin, P. Chiang, W. Chuang, Y. Liu, H. Hsu, W. Hung, W. Tang, K. Wong and P. Chou, Probe exciplex structure of highly efficient thermally activated delayed fluorescence organic light emitting diodes, *Nat. Commun.*, 2018, **9**, 3111.

13 X. Liu, H. Popli, O. Kwon, H. Malissa, X. Pan, B. Park, B. Choi, S. Kim, E. Ehrenfreund, C. Boehme and Z. V. Vardeny, Isotope Effect in the Magneto-Optoelectronic Response of Organic Light-Emitting Diodes Based on Donor–Acceptor Exciplexes, *Adv. Mater.*, 2020, **32**, 2004421.

14 H. Lim, H. Shin, K. Kim, S. Yoo, J. Huh and J. Kim, An Exciplex Host for Deep-Blue Phosphorescent Organic Light Emitting Diodes, *ACS Appl. Mater. Interfaces*, 2017, **9**, 37883–37887.

15 J. W. Sun, J. Lee, C. Moon, K. Kim, H. Shin and J. Kim, A Fluorescent Organic Light-Emitting Diode with 30% External Quantum Efficiency, *Adv. Mater.*, 2014, **26**, 5684–5688.

16 S. Kim, W. Jeong, C. Mayr, Y. Park, K. Kim, J. Lee, C. Moon, W. Brütting and J. Kim, Organic Light-Emitting Diodes with 30% External Quantum Efficiency Based on a Horizontally Oriented Emitter, *Adv. Funct. Mater.*, 2013, **23**, 3896–3900.

17 G. Liu, H. Sasabe, K. Kumada, A. Matsunaga, H. Katagiri and J. Kido, Facile synthesis of multi-resonance ultra-pure-green TADF emitters based on bridged diarylamine derivatives for efficient OLEDs with narrow emission, *J. Mater. Chem. C*, 2021, **9**, 8308–8313.

18 X. Liang, Z. P. Yan, H. B. Han, Z. G. Wu, Y. X. Zheng, H. Meng, J. L. Zuo and W. Huang, Peripheral amplification of multi-resonance induced thermally activated delayed fluorescence for highly efficient OLEDs, *Angew. Chem., Int. Ed.*, 2018, **57**, 11316–11320.

19 S. K. Jeon and J. Y. Lee, Highly efficient exciplex organic light-emitting diodes by exciplex dispersion in the thermally activated delayed fluorescence host, *Org. Electron.*, 2020, **76**, 105477.

20 H. L. Lee, K. H. Lee and J. Y. Lee, Stable hole transport type host boosting the efficiency and lifetime of the exciplex host based phosphorescent organic light-emitting diodes, *Dyes Pigm.*, 2019, **171**, 107714.

21 Q. Wang, Y. Tao, X. Qiao, J. Chen, D. Ma, C. Yang and J. Qin, High-Performance, Phosphorescent, Top-Emitting Organic Light-Emitting Diodes with p–i–n Homojunctions, *Adv. Funct. Mater.*, 2011, **21**, 1681–1686.

22 P. Freitag, S. Reineke, S. Olthof, M. Furno, B. Lüssem and K. Leo, White top-emitting organic light-emitting diodes with forward directed emission and high color quality, *Org. Electron.*, 2010, **11**, 1676–1682.

23 C. H. Park, H. J. Lee, J. H. Hwang, K. N. Kim, Y. S. Shim, S. Jung, C. H. Park, Y. W. Park and B. Ju, High-Performance Hybrid Buffer Layer Using 1,4,5,8,9,11- Hexaazatriphenylenehexacarbonitrile/Molybdenum Oxide in Inverted Top-Emitting Organic Light-Emitting Diodes, *ACS Appl. Mater. Interfaces*, 2015, **7**, 6047–6053.

24 W. Y. Park, H. W. Cheong, C. Lee and K. W. Whang, Design of highly efficient RGB top-emitting organic light-emitting diodes using finite element method simulations, *Opt. Express*, 2016, **24**, 24018–24031.

25 S. Hofmann, M. Thomschke, P. Freitag, M. Furno, B. Lüssem and K. Leo, Top-emitting organic light-emitting diodes: Influence of cavity design, *Appl. Phys. Lett.*, 2010, **97**, 253308.

26 Z. B. Wang, M. G. Helander, J. Qiu, D. P. Puzzo, M. T. Greiner, Z. M. Hudson, S. Wang, Z. W. Liu and Z. H. Lu, Unlocking the full potential of organic light-emitting diodes on flexible plastic, *Nat. Photonics*, 2011, **5**, 753–757.

27 K. A. Neyts, Simulation of light emission from thin-film microcavities, *J. Opt. Soc. Am. A*, 1998, **15**, 962–971.

28 R. Meerheim, M. Furno, S. Hofmann, B. Lüssem and K. Leo, Quantification of energy loss mechanisms in organic light-emitting diodes, *Appl. Phys. Lett.*, 2010, **97**, 253305.

29 J. Lee, T. Han, M. Park, D. Y. Jung, J. Seo, H. Seo, H. Cho, E. Kim, J. Chung, S. Choi, T. Kim, T. Lee and S. Yoo, Synergetic electrode architecture for efficient graphene-based flexible organic light-emitting diodes, *Nat. Commun.*, 2016, **7**, 11791.

30 Y. H. Chen, Q. Wang, J. S. Chen, D. G. Ma, D. H. Yan and L. X. Wang, Organic semiconductor heterojunctions as charge generation layers and their application in tandem organic light-emitting diodes for high power efficiency, *Org. Electron.*, 2012, **13**, 1121–1128.

31 T. Fleetham, J. Ecton, G. Li and J. Li, Improved out-coupling efficiency from a green microcavity OLED with a narrow band emission source, *Org. Electron.*, 2016, **37**, 141–147.

32 T. Schwab, S. Schubert, S. Hofmann, M. Fröbel, C. Fuchs, M. Thomschke, L. Müller-Meskamp, K. Leo and M. C. Gather, Highly Efficient Color Stable Inverted White Top-Emitting OLEDs with Ultra-Thin Wetting Layer Top Electrodes, *Adv. Opt. Mater.*, 2013, **1**, 707–713.

33 S. D. Yambem, M. Ullah, K. Tandy, P. L. Burn and E. B. Namdas, ITO-free top emitting organic light emitting diodes with enhanced light out-coupling, *Laser Photonics Rev.*, 2014, **8**, 165–171.

34 S. Park, J. T. Lim, W. Jin, H. Lee, B. Kwon, N. S. Cho, J. Han, J. Kang, S. Yoo and J. Lee, Efficient Large-Area Transparent OLEDs Based on a Laminated Top Electrode with an Embedded Auxiliary Mesh, *ACS Photonics*, 2017, **4**, 1114–1122.

35 Y. Chen, W. Lee, Y. Chen, C. Lin, S. Wen, M. Jiao, G. Su, H. Y. Lin, R. J. Visser, B. L. Kwak, C. Chen, W. Lin, S. Wang, C. Chang and C. Wu, A Vision toward Ultimate Optical Out-Coupling for Organic Light-Emitting Diode Displays: 3D Pixel Configuration, *Adv. Sci.*, 2018, **5**, 1800467.
36 C. X. Zang, S. H. Liu, M. X. Xu, R. F. Wang, C. Cao, Z. L. Zhu, J. M. Zhang, H. Wang, L. T. Zhang, W. F. Xie and C. S. Lee, Top-emitting thermally activated delayed fluorescence organic light-emitting devices with weak light-matter coupling, *Light: Sci. Appl.*, 2021, **10**, 116.
37 S. H. Liu, C. X. Zang, J. M. Zhang, S. Tian, Y. Wu, D. Shen, L. T. Zang, W. F. Xie and C. S. Lee, Air-stable Ultrabright Inverted Organic Light-emitting Devices With Metal Ion-chelated Polymer Injection Layer, *Nano-Micro Lett.*, 2022, **14**, 14.